Electronic Supplementary Material (ESI) for Physical Chemistry Chemical Physics.

Supplemental Information to the Manuscript

Computational Insights into CdSe Quantum Dots' Interactions with Acetate Ligands

Patrick K. Tamukong, Wadumesthrige D. N. Peiris, and Svetlana Kilina*

Department of Chemistry and Biochemistry, North Dakota State University, Fargo, North Dakota 58108-6050, United States

Calculations of Binding Energy **between the QD and a Ligand.** To identify the strength of the interaction between the QD and a ligand, the ligand-QD binding energies are computed for all four cases both in vacuum and in acetonitrile solvent for the $(CdSe)_{33}$ covered by 1 to 10 ligands. For cases **1**, **2**, and **4**, the following formula is used in computing an averaged ligand-QD binding energy (E_b):

$$\langle E_b \rangle = \frac{\left[E^{opt}(QD + Ligands)\right] - \left[E^{opt}(QD) + N \times E^{opt}(Ligand)\right]}{N}. \tag{1}$$

Here N denotes the number of ligands in cases **1**, **2** and **4**. The first term in Eq. 1 stands for the total energy of the optimized $(CdSe)_{33}$ covered by ligands. The last two terms are defined by the total energy of the optimized structure of the bare $(CdSe)_{33}$ and the isolated ligand, respectively, where the last is either the acetate or cadmium acetate for cases **1** or **2**, and $[Cd^{2+}(CH_3COO^-)_2]$ complex for the case **4**. In case **3**, we use the slightly modified formula:

$$\langle E_b \rangle = \frac{\left[E^{opt}(QD + Ligands)\right] - E^{opt}(QD) - {}^{N}\!/_{2}\left[E^{opt}(Ligand_1) + E^{opt}(Ligand_2)\right]}{{}^{N}\!/_{2}}, \tag{2}$$

where the last two terms denote the total energy of the isolated acetate ($ligand_1$) and the cadmium acetate ($ligand_2$), while N/2 equals to the number of acetate and cadmium acetate pairs. Note that $\langle E_b \rangle$ in Eq. 1 and 2 does not indicate the energy per bond formed by each ligand but rather the average energy per ligand, irrespective of the mode of binding and the QD's surface at which the ligand is attached. Alternatively, we calculate the ligand-QD binding energy for a specific ligand as follows:

$$E_b = \left[E^{opt}\left(QD + (N)Ligands\right)\right] - \left[E^{opt}\left(QD + (N-1)Ligands\right)\right] - E^{opt}\left(Ligand\right) \qquad (3)$$

$$E_b = \frac{\left[E^{opt}\left(QD + (N)Ligands\right)\right] - \left[E^{opt}\left(QD + (N-2)Ligands\right) + E^{opt}(Ligand_1) + E^{opt}\left(Ligand_2\right)\right]}{2} \qquad (4)$$

Similar to Eqs. 1 and 2, the first term in Eqs. 3 and 4 denotes the total energy of the optimized $(CdSe)_{33}$ QD covered by N ligands. In Eq. 3, the last two terms are defined by the total energy of the ligated QD with one cut ligand and the total energy of the isolated ligand for cases **1**, **2**, and **4**. For the case **3**, we use Eq. 4, where the second term stands for the ligated QD with one lost pair of CH_3COO^- and $[Cd^{2+}(CH_3COO^-)]$ ligands (2 lost ligands) and the last two terms are defined by the total energy of the isolated acetate ($ligand_1$) and cadmium acetate ($ligand_2$).

Note, the ligand passivation is done starting with covering facets **A** and **D** and then systematically adding ligands to facets **B** and **C**. For example, for cases **1** to **4** with 10 ligands, facets **A** and **D** each bare 3 ligands while **B** and **C** have a ligand pair each.

QD-Ligand Interactions: Effect of the Ligand Binding Mode and the QD's Surface. Binding energies of the ligand for cases **1**, **2**, and **3** with ligand attached to the **A** surface of the QD through different modes (**M**, **Ch**, and **Bg**) are compared in Figure S1 (a) and (b) in vacuum and CH_3CN solvent, respectively. In vacuum, the bridging mode provides the most stable binding energy for case **1** (-4.54 eV) and **3** (-5.07 eV), whereas the lowest energy configuration for case **2** is the chelating mode (-3.68 eV). Contrarily, cases **1** and **3** found the chelating mode to be the least stable. In addition, case **3** results in the most stable conformations among all binding modes in vacuum. This can be rationalized by overall neutrality of the system **3**, where the ligand pair of the acetate (with -1 charge) and cadmium acetate (with +1 charge) mutually compensates each other, stabilizing the energy of the ligated QD. In contrast, the QD interacting with the positively charged species – cadmium acetate (case **2**) – is the least stable, especially at its monodentate and bridging attachment modes. However, the polar solvent drastically changes this trend, making the QD ligated by the cadmium acetate (case **2**) the most stable among all. However, the polar solvent also significantly weakens the QD-ligand interactions for all cases, resulting in the absolute value of the binding energy being at the ranges of 1.0-0.7 eV, which is three to five times smaller than those in vacuum. This is expected since the considered systems have a strong electrostatic dipole moment, which is screened out by a polar solvent.

In the presence of the acetonitrile solvent, the bridging mode becomes the most stable for all three cases, with the difference in binding energies between ligand cases being slightly less than 0.1 eV. In the polar solvent, the monodentate mode is the least favorable attachment for cases **2** and **3** (differs by ~0.15 eV and ~0.05 eV from the bridging and chelating modes, respectively), while it is nearly as stable as the chelating mode (at the order of thermal fluctuations) for case **1**. As such, we conclude that the bridging mode is the most probable attachment of either acetate or cadmium acetate to the CdSe surface. Therefore, we use the bridging mode of ligand attachment for all further calculations.

The **A** layer is expected to be one of the most reactive surfaces for $(CdSe)_{33}$, and our calculations demonstrate that this is indeed the case for ligands **1** and **3** both in vacuum and solvent, as illustrated in Figure S1 (c) and (d). However, **A** is the least reactive surface for case **2**. Instead, **D** and **C** layers provide the most stable binding to the cadmium acetate cation, with **D** being the most reactive in vacuum and **C** is in solvent. Presence of both Se and Cd ions at the same **D**-surface is responsible for an increase in its interaction with the cadmium acetate cation, because it provides an opportunity for Cd^{2+} to interact with the surface Se and O to bind to the surface Cd.

Interestingly, the polar solvent strongly stabilizes the interaction of the QD with cadmium acetate for all facets, making case **2** the most stable among all ligands irrespective of the interacting surface. Such a strong interaction of **2** is likely due to the ionic nature of the Se-Cd bond formed between the CdSe QD and the cadmium acetate cation, which stabilizes the structure in a polar solvent. In fact, the Mulliken atomic charge on the Cd^{2+} of cadmium acetate ligand is much more sensitive to the solvent increasing by 1.4-1.8 times in acetonitrile solvent as compared to vacuum, while the charge insignificantly changes for oxygens in acetate groups (Table S1). Moreover, in case **2** in solution, the charge on Cd^{2+} is found to be at least 0.1 a.u. greater than those in case **3**, although the values for the O-atoms bearing the Cd^{2+} are relatively similar (Table S1). This is because an additional acetate group bound to the QD surface perturbs the charge on cadmium acetate and, thus, weakens the ionic Cd-Se bond at the QD surface in case **3**. Note that the bond weakening in case **3** is more pronounced in a polar solvent than in vacuum because of stronger delocalization of the charge density in the presence of the solvent, resulting in weaker QD-ligand interaction than those in case **2**. Overall, solvent effects are seen to be dramatic, diminishing the ligand binding strength for all cases and reversing binding preferences, due to the strong screening of the dipole-dipole intercations by the polar media.

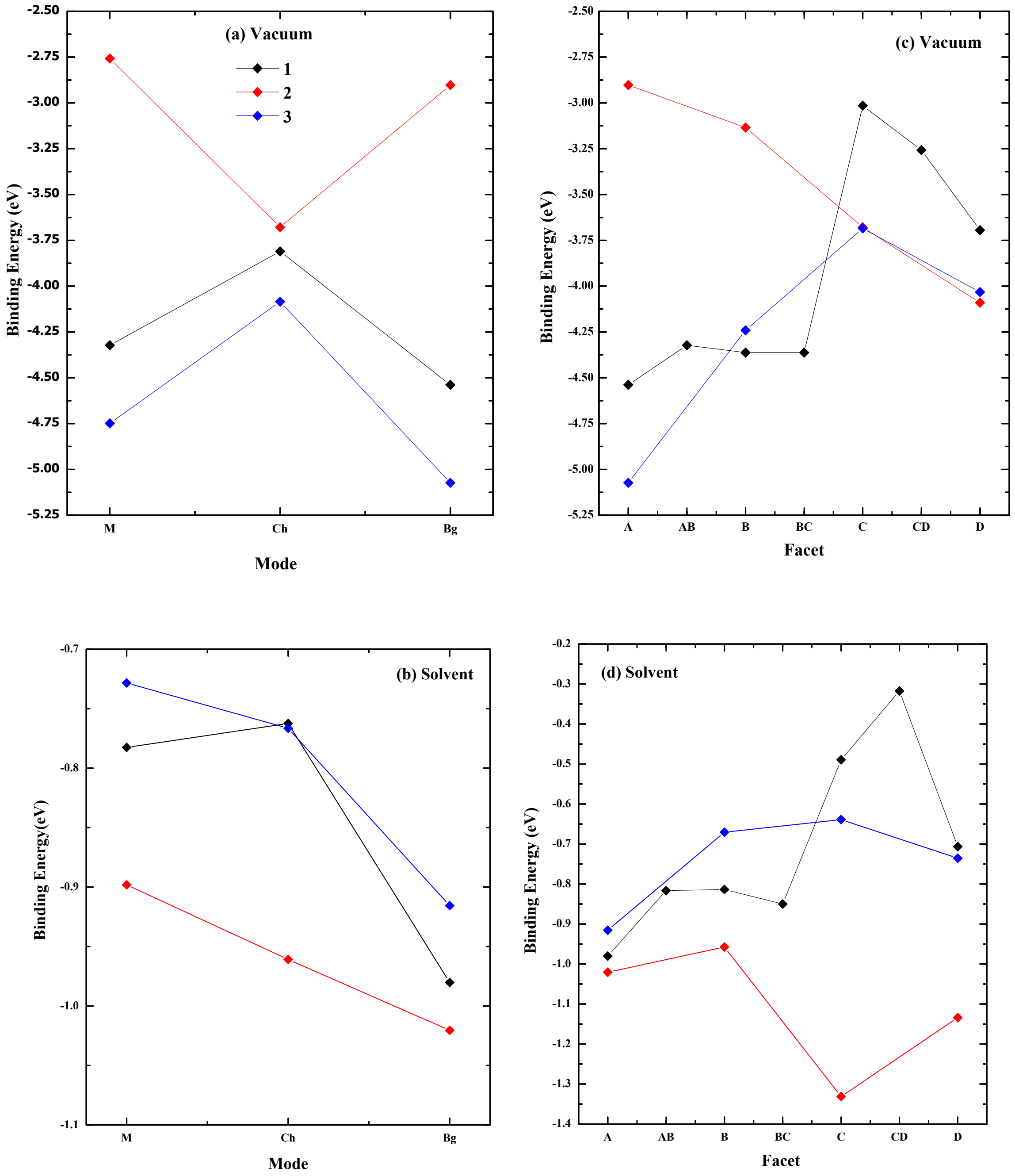

Figure S1: QD-ligand binding energies for acetate and cadmium acetate ligands interacting at various attachment modes and at different facets of the $(CdSe)_{33}$ QD. Ligand cases **1** (black line), **2** (red line), and **3** (blue line) bound to the facet **A** at three different attachment modes – monodentate (**M**), chelating (**Ch**), and bridging (**Bg**) – in vacuum (a), and (b) acetonitrile solvent. Ligand cases **1**, **2**, and **3** attached at their bridging mode to various QD facets in vacuum (c) and acetonitrile solvent (d). For all cases in solvent, the bridging mode provides the most stable ligand attachment, while **A** (cases **1** and **2**) and **C** layers (case **3**) with 2-coordinated Cd are the most reactive QD's surfaces in the polar solvent.

Table S1. Mulliken charges (a.u.) on Oxygen atoms of the acetate ligand and the extra Cd^{2+} (for cadmium acetate ligand) for ligand cases **1A**, **2A**, and **3AA**.

	1A		**2A**		**3AA**	
	Vacuum	**Solvent**	**Vacuum**	**Solvent**	**Vacuum**	**Solvent**
O	-0.486817	-0.479981	-0.507791	-0.459550	-0.449162	-0.458548
O	-0.425874	-0.481869	-0.436705	-0.506249	-0.468946	-0.509121
Cd^{2+}	-	-	0.714603	1.253892	0.850757	1.153554
O					-0.496612	-0.471736
O					-0.425076	-0.490449

Table S2. Average binding energy per ligand for Cases **1**, **2**, **3**-LSF (same surface), **3-**YLDF (different surfaces), and **4**, computed for up to 10 ligands attached to $(CdSe)_{33}$ in vacuum and in acetonitrile solvent using Equations 3 and 4 (shown in the paper). All energies are in eV.

# of Ligands (Y)	Case Type				
	1	2	3-LSF	3-LDF	4
			Vacuum		
1	-4.54	-2.90	-	-	-
2	-2.56	-2.68	-5.07	-4.66	-1.44
4	1.41	1.57	-5.03	-5.03	-1.70
6	4.69	4.27	-5.53	-5.28	-1.58
8	7.71	5.26	-4.58	-5.44	-1.62
10	9.54	8.17	-5.81	-4.68	-1.64
			Solvent		
1	-0.98	-1.02	-	-	
2	-0.68	-0.51	-0.92	-0.89	-0.40
4	-0.24	-0.62	-0.79	-0.84	-0.68
6	-0.15	-0.50	-0.78	-0.79	-0.46
8	-0.25	-0.63	-1.35	-1.33	-0.86
10	-0.14	-0.82	-0.58	-0.85	-0.46

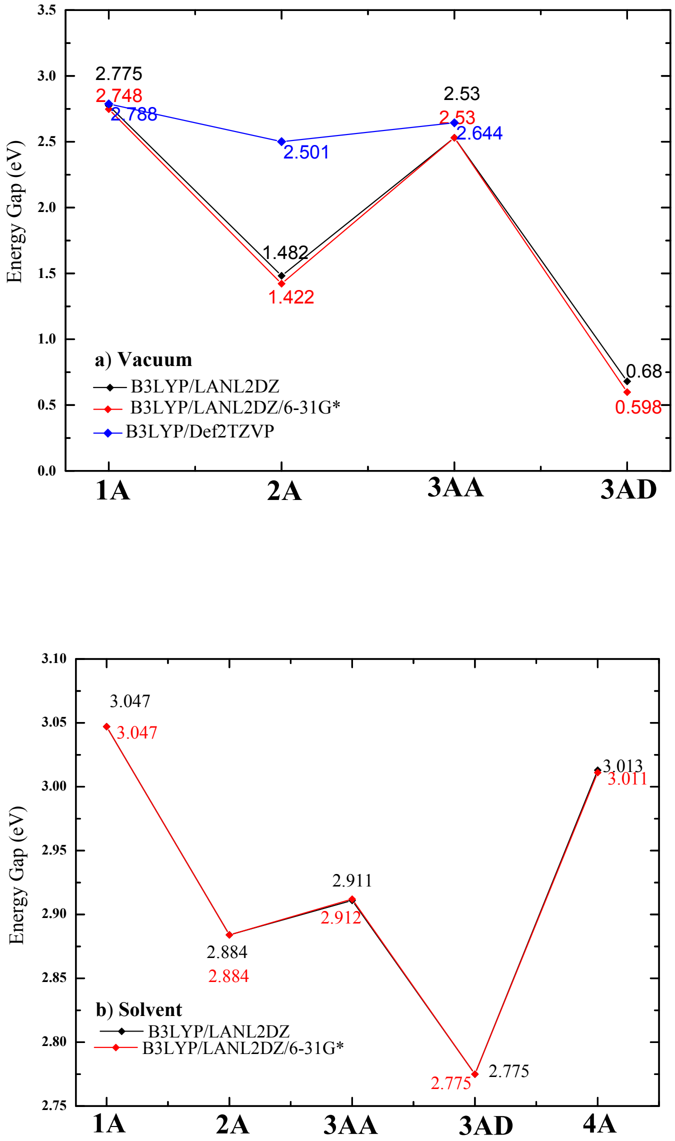

Figure S2. Energy gaps for ligated $(CdSe)_{33}$ by **1A**, **2A**, **3AA**, and **3AD** ligands calculated with the B3LYP functional and Def2-TZVP (blue line), LANL2DZ (black lines), and LANL2DZ/6-31G* (red lines) basis sets (where 6-31G* was used only for ligand atoms and LANL2DZ for QD atoms). The curves in (a) were obtained in vacuum, and those in (b) in acetonitrile solvent when geometry is also optimized in the same solvent using the same basis sets. Only in the case **2A** there is significant deviation in the energy gaps when calculated by the larger basis set Def2-TZVP. This is because the geometry optimization of 2A using smaller basis set, LANL2DZ or

LANL2DZ/6-31G*, results in different structural conformation, compared to those obtained by Def2-TZVP. As a result, there are no ligand-localized mid-gap states in **2A** when it is calculated by Def2-TZVP that significantly increases the energy gap.

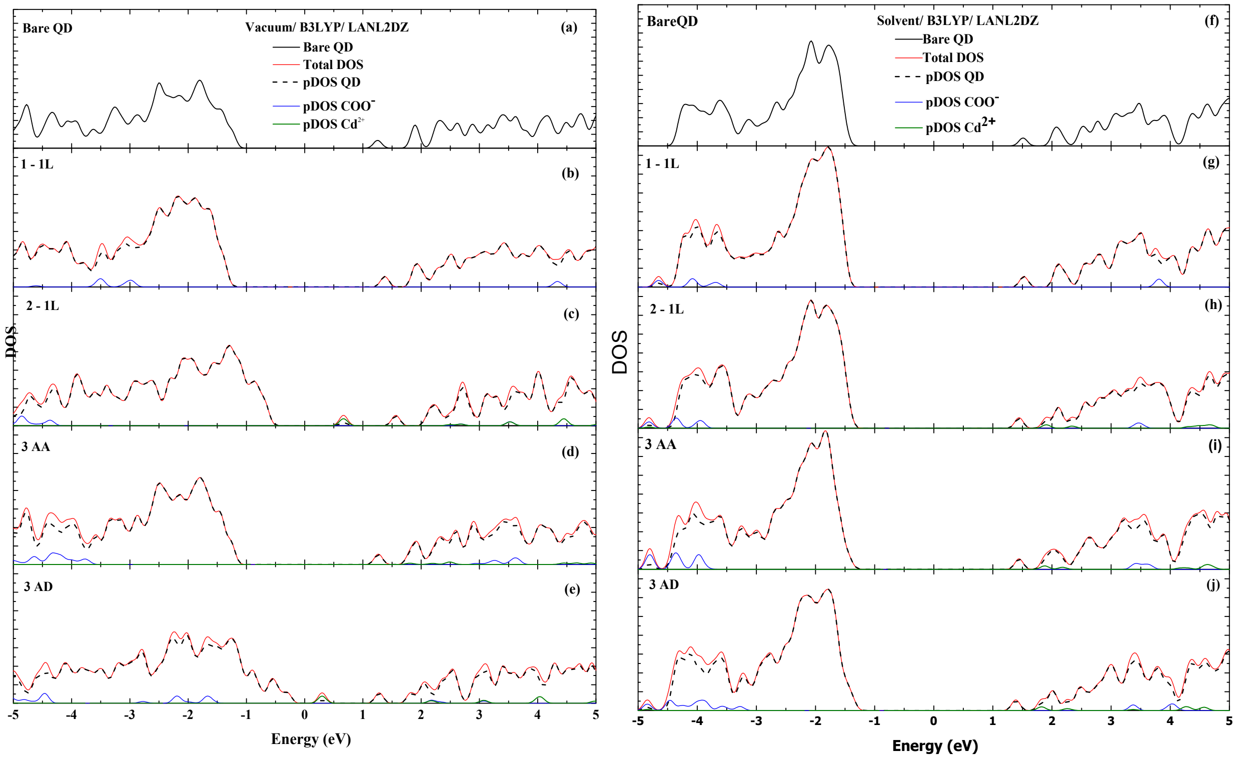

Figure S3. Density of States (DOS) and projected DOS (pDOS) of ligated $(CdSe)_{33}$ QDs for the following cases: (a) bare QD; (b) **1A**; (c) **2A**; (d) **3AA**; and (e) **3AD**. Calculations were done using the B3LYP functional and LANL2DZ basis set in vacuum (left panel) and in acetonitrile solvent (right panel). The solid black line indicates the DOS of the bare QD; the red line represents the total DOS of the ligated QD; the dashed black line represents the pDOS of the QD; the blue line is for the pDOS of acetate groups; whereas the green line indicates the pDOS of Cd^{2+} ion in the cadmium acetate.

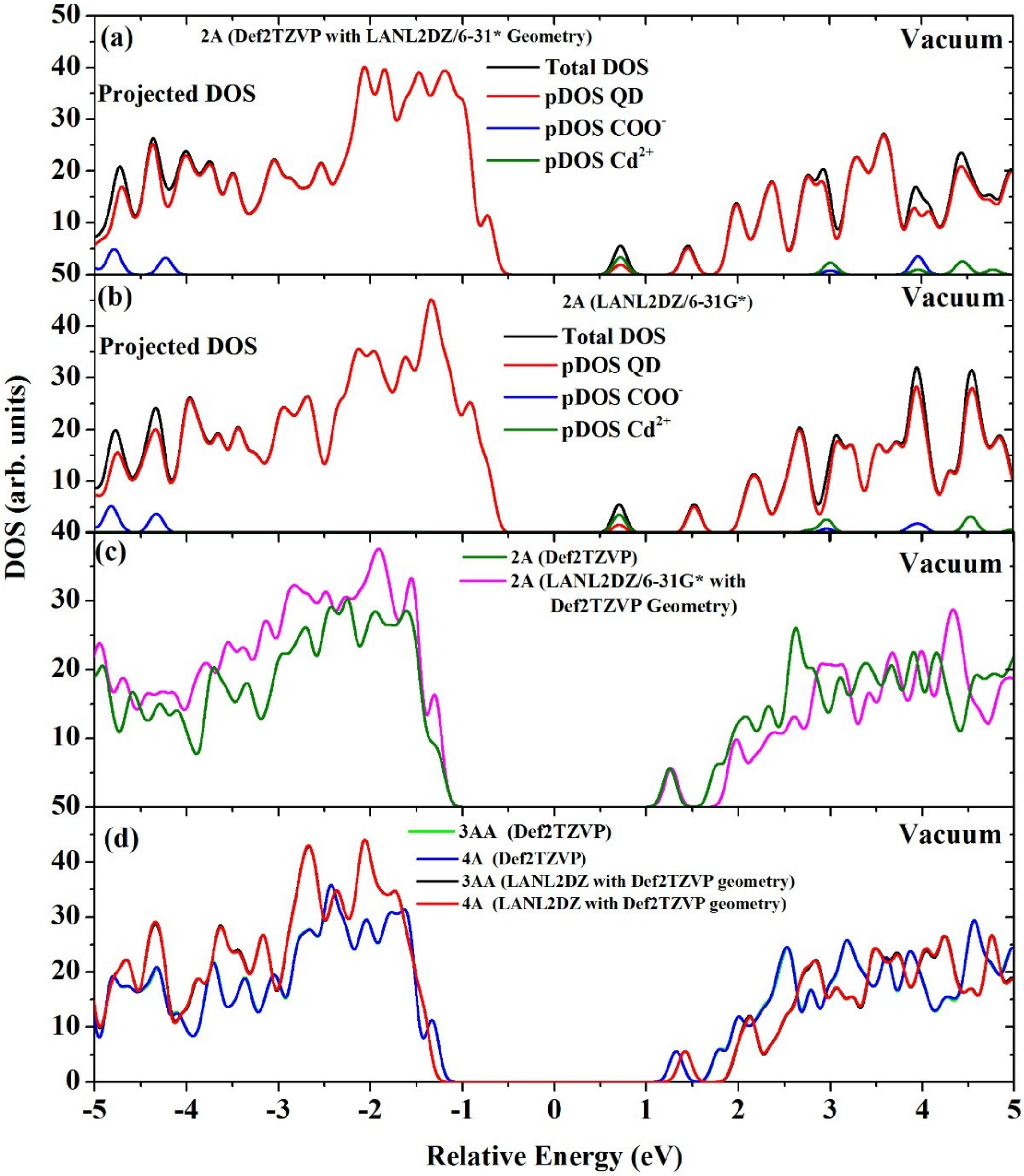

Figure S4. Density of States (DOS) and projected DOS (pDOS) of ligated $(CdSe)_{33}$ QDs for the **2A**, **3AA**, and **4A** ligand cases. The electronic structure of **2A** is done in vacuum using the B3LYP functional and Def2-TZVP basis based on the geometry optimized by B3LYP// LANL2DZ/6-31G* **(a)** and compared to those where both the geometry and DOS are obtained either with the B3LYP//LANL2DZ/6-31G* **(b)** or with B3LYP//Def2-TZVP **(c)**; similar data but for **3AA** and **4A** **(d)**. For the same methodology, the DOS of **3AA** and **4A** completely coincide (green with blue lines and black with red lines in **(d)**). For all ligand cases, the larger Def2-TZVP basis set has a miner effect on the DOS – slightly increases the energy gap and insignificantly distorts main bands – when the same geometry is used. However, the structure **2A** obtained by Def2-TZVP has no mid-gap trap states, in contrast to those obtained by LANL2DZ/6-31G* basis set.

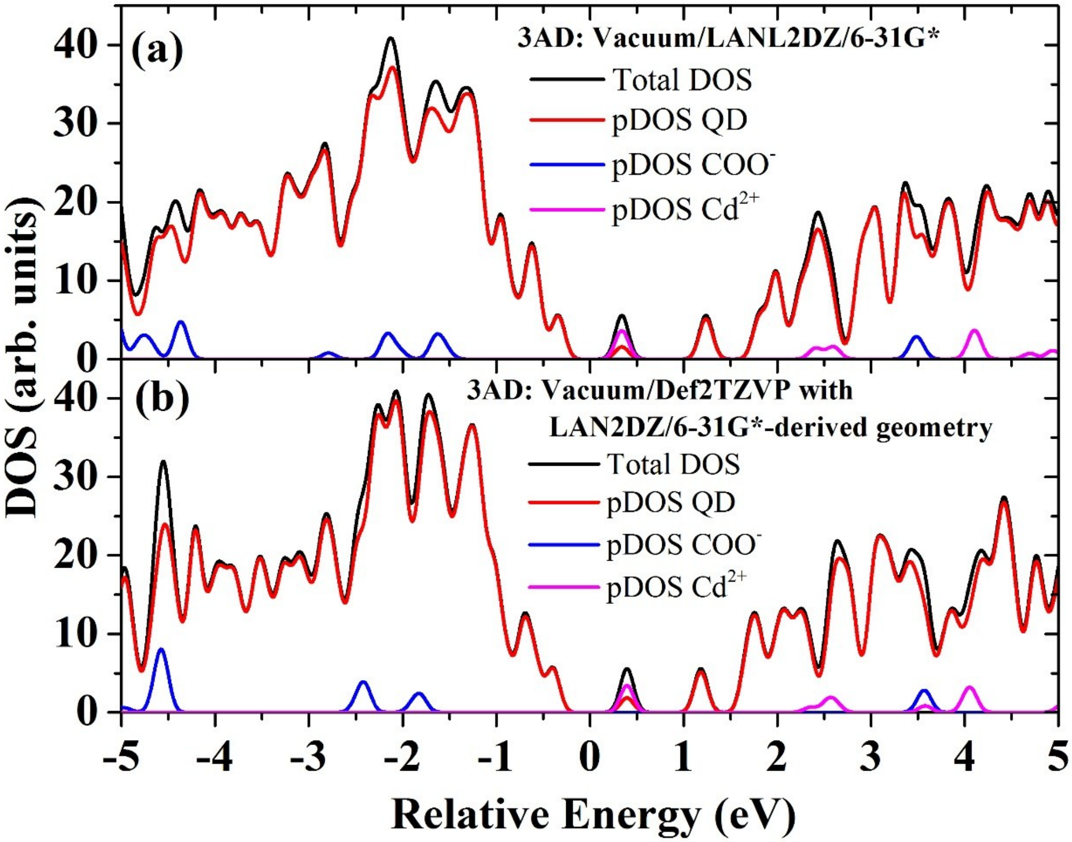

Figure S5. The projected DOS (pDOS) of **3AD** ligated $(CdSe)_{33}$ QDs. The electronic structure of **3AD** is done in vacuum using the B3LYP functional and Def2-TZVP basis based on the geometry optimized by B3LYP//LANL2DZ/6-31G* **(a)** and compared to those where the DOS is calculated by B3LYP//LANL2DZ/6-31G* based on the geometry obtained by B3LYP//Def2-TZVP **(b)**. These two sets of pDOS show no significant topological differences pointing on insignificant effect of the larger basis set such as Def2-TZVP on the electronic structure of the ligated QD, when the same geometry is used.

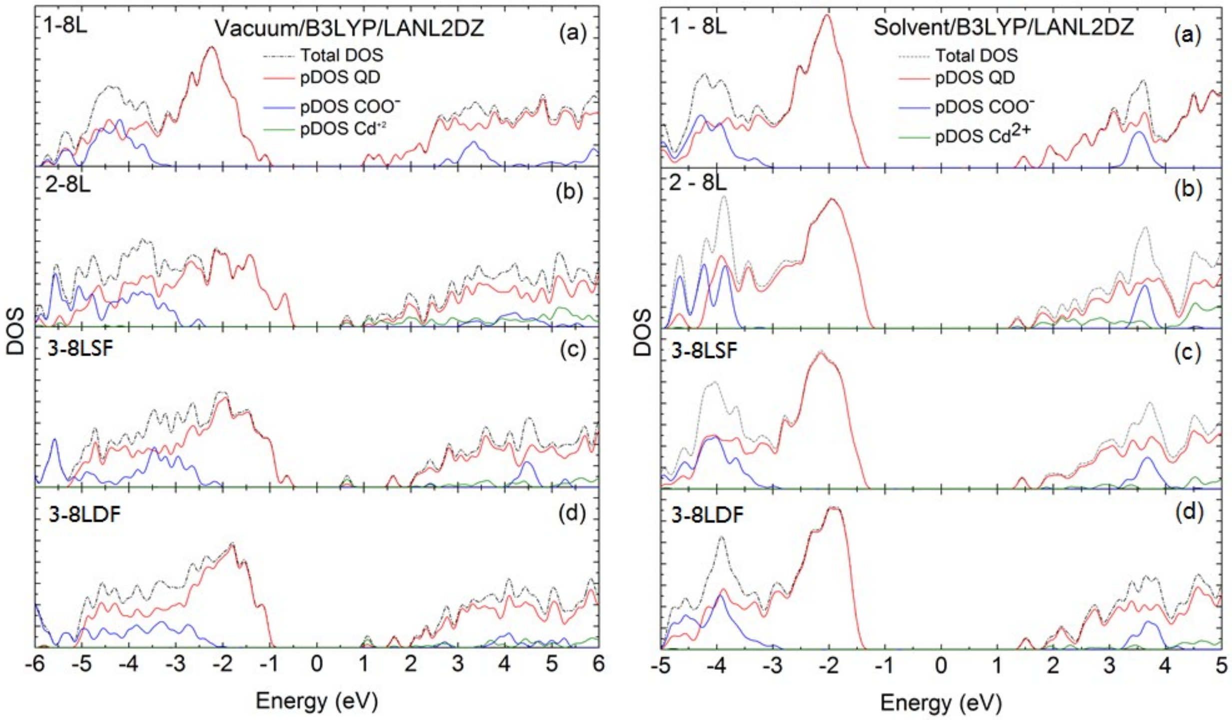

Figure S6. Density of States (DOS) and projected DOS (pDOS) of $Cd_{33}Se_{33}$ QD with 8 bound ligands for the following cases: (a) **1-8L**, (b) **2-8L**, (c) **3-8LSF**, and (d) **3-8LDF**. Calculations were done with B3LYP/LANL2DZ in vacuum (left panel) and acetonitrile solvent (right panel). The dashed black line represents the total DOS of the system; the solid red line is the pDOS of the QD; the blue line is for the pDOS of acetate groups; whereas, the green line indicates the pDOS of the Cd^{2+} in cadmium acetate in cases **2-8L**, **3-8LSF**, and **3-8LDF**. In all ligand cases, the polar solvent opens the gap shifting the Cd^{2+}-associated orbitals inside in the conduction band of the QD.

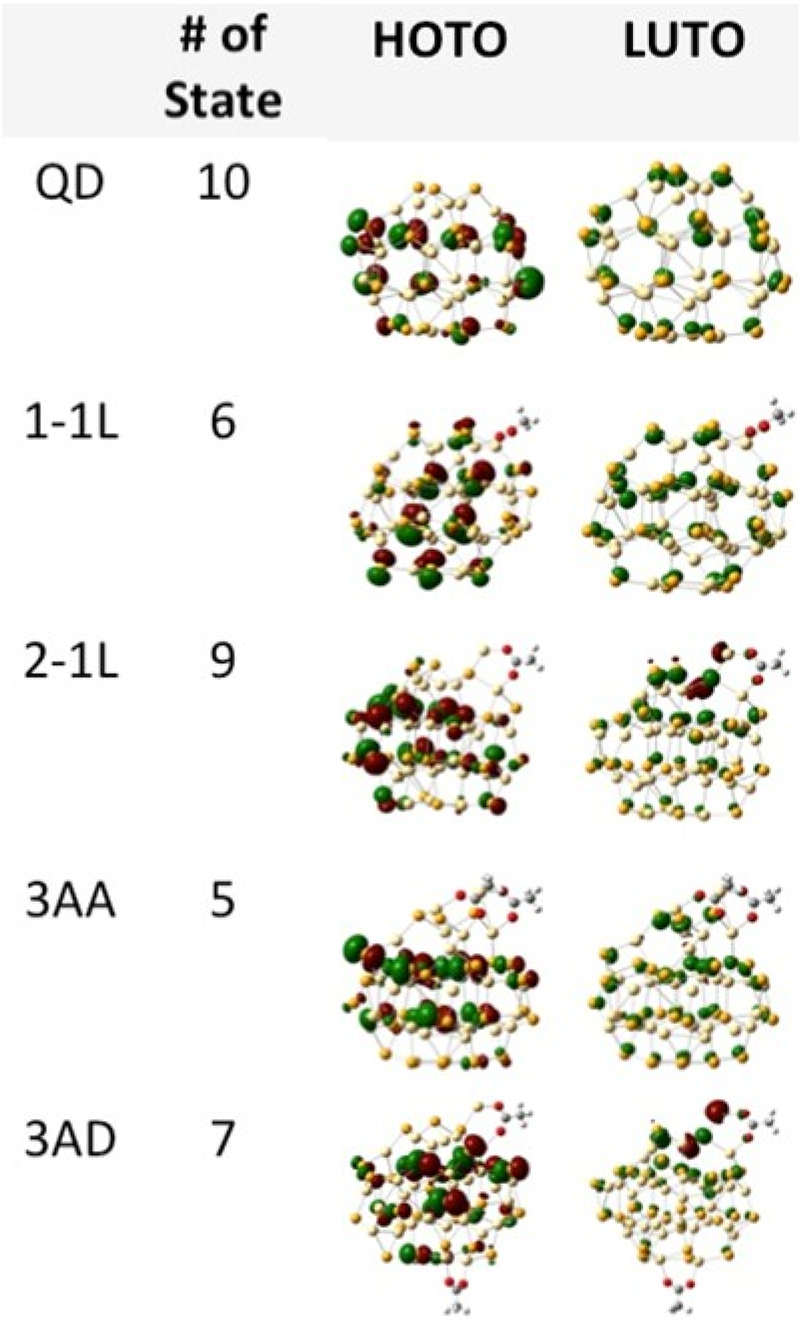

Figure S7. Natural transition orbitals (NTOs) contributing to the most intense optical transitions for ligand cases **1A**, **2A**, **3AA**, and **3AD** in acetonitrile solvent. The corresponding transition states are also included. HOTO stays for hole and LUTO for electron pairs contributing to the optical transition. Calculations are done using geometries optimized in CH_3CN.

	HOTO	**LUTO**
	Vacuum Geometry	
1A	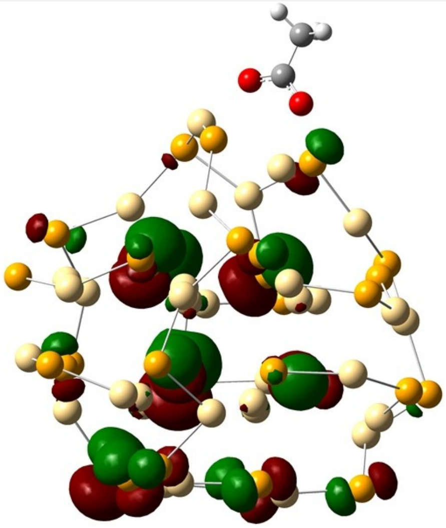	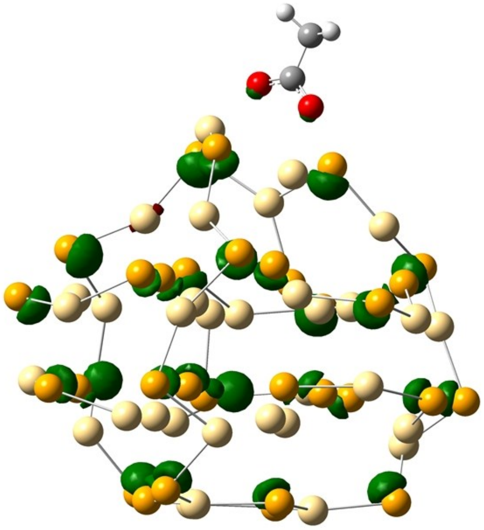
	Solvent Geometry	
1A	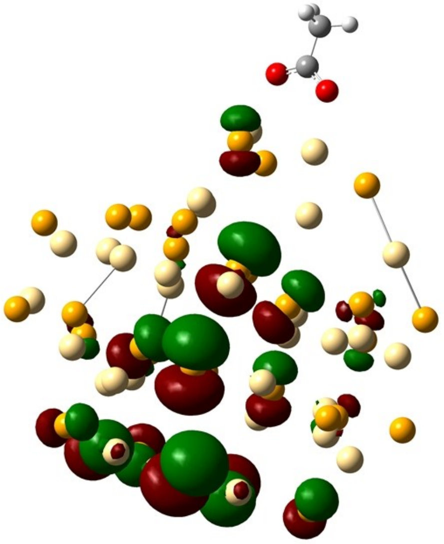	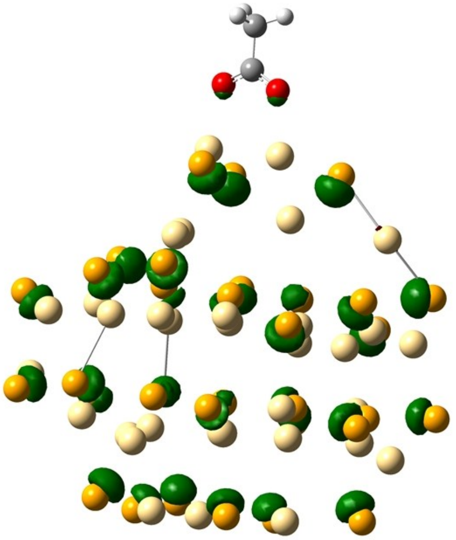

Solvent Geometry	**HOTO**	**LUTO**
2A	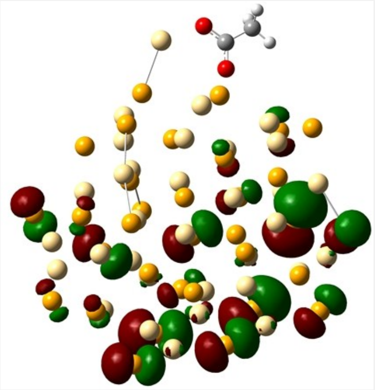	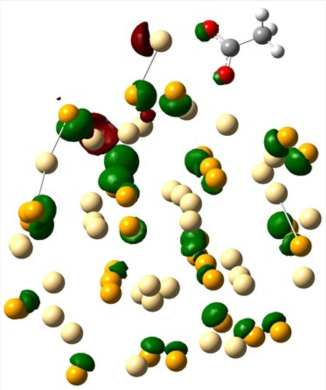
3AA	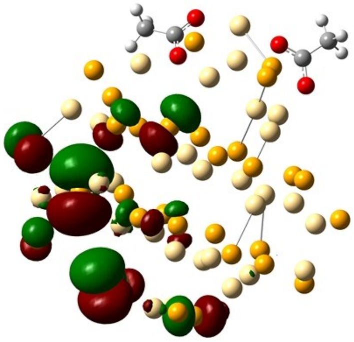	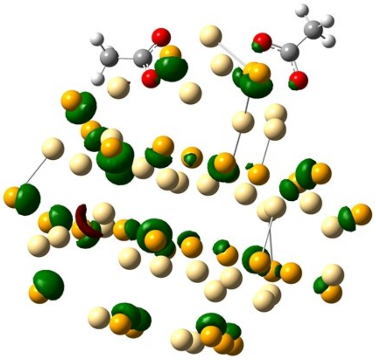
3AD	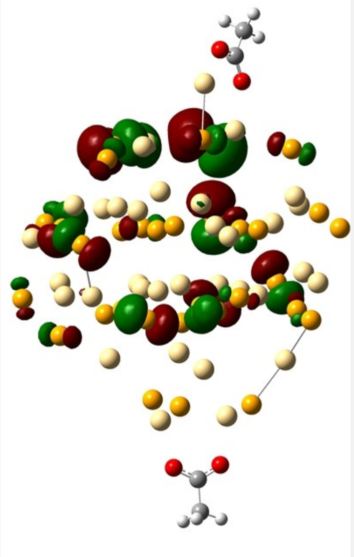	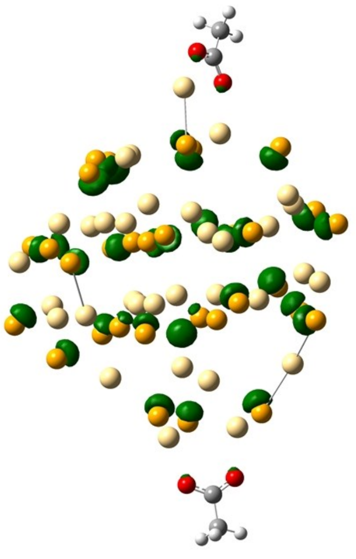

Figure S8. Natural transition orbitals (NTOs) contributing to the lowest energy optical transitions for case **1A** with vacuum-optimized geometry and of cases **1A**, **2A**, **3AA**, and **3AD** with solvent-optimized geometry. All NTOs were obtained for spectra obtained in solution as shown in Figure 6.

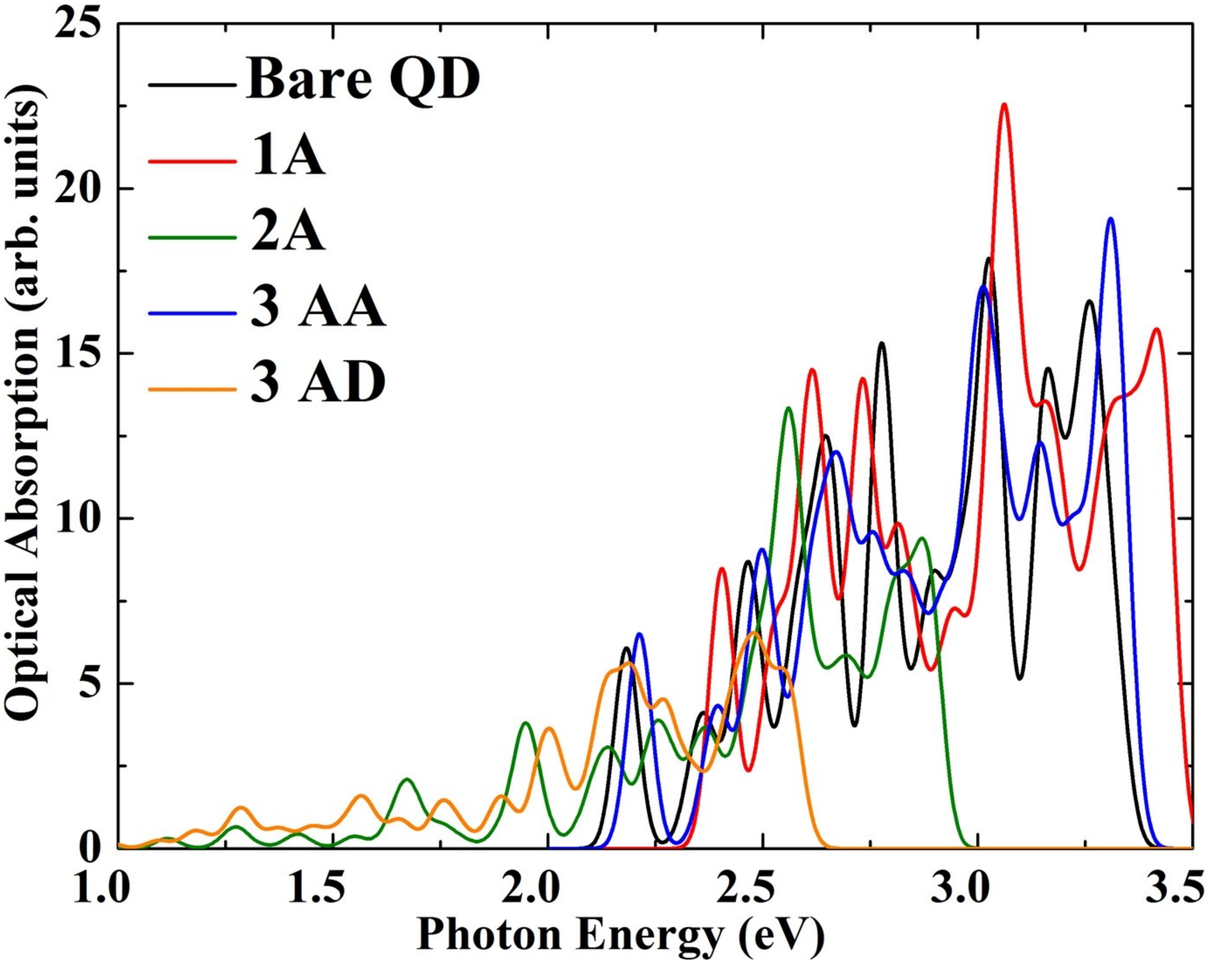

Figure S9: Absorption spectra of bare and ligated $Cd_{33}Se_{33}$ QDs for the ligand cases: **1A**; **2A**; **3AA**; and **3AD**. Calculations were done using B3LYP/LANL2DZ with TDDFT in vacuum and using previously vacuum-optimized geometries. As shown in the legends, the black line represents the spectrum of the bare $Cd_{33}Se_{33}$ QD; whereas the red, green, blue, and cyan lines are for cases **1A**, **2A**, **3AA**, and **3AD**, respectively.

When both geometries and absorption spectra are calculated in vacuum, the lowest energy transition in all ligand cases is much less intensive (having the oscillator strength of 0.03 or less) and noticeably red shifted (especially for **2A**), while the overall spectra are topologically different, as can be seen in Figure S9 in Supplemental Information. It should be recalled that the extra Cd^{2+} introduces ligand-localized midgap states in this case resulting in the dark or semi-dark lower energy transitions with a charge transfer character (QD-to-ligand). Thus, a polar solvent has a drastic effect on the electronic structures and, consequently, on absorption spectra of both ligated and the bare QD: acetonitrile solvent strongly blue-shifts and modifies the absorption spectra while it ‘brightens’ optical transitions due to enhancement in delocalization character of orbitals contributing to these transitions.